11-4-2008

Sedimentation of Organic - Inorganic Composites by Optical Turbidity

Reshma K. Harrinauth
University of South Florida

Sedimentation of Organic - Inorganic Composites by Optical Turbidity

by

Reshma K. Harrinauth

A thesis submitted in partial fulfillment
of the requirements for the degree of
Master of Science in Chemical Engineering
Department of Chemical and Biomedical Engineering
College of Engineering
University of South Florida

Major Professor: Vinay K. Gupta, Ph.D.
Scott Campbell, Ph.D.
Babu Joseph, Ph.D.

Date of Approval:
November 4, 2008

Keywords: settling velocity, turbidometer, titania, ceria, pnipam

DEDICATION

To my family

ACKNOWLDEGEMENTS

I would like to express sincere gratitude and thanks to Dr Vinay K. Gupta who has offered invaluable assistance, guidance and support throughout the time it took for me to complete my research and thesis. I would also like to thank my committee members, Dr Babu Joseph and Dr Scott Campbell, who have been integral in my education at the University of South Florida. I would also like to thank the members of my research lab, David Walker, Fadena Fanord, Bijith Mankidy and Chhavi Manocha, who has been a constant source of knowledge and assistance. I would like to give a special thanks to my lab mate, Cecil Coutinho without his guidance and support this thesis would not be possible. My thank to the many friends I have made at USF especially, Nada Elsayed and Brandon Smeltzer, they have proven our friendship would last a lifetime. I would like to thank my extended family, for their support, love and encouragement in the pursuit of my education. Finally to my parents and sister, without their support, unconditional love and sacrifice this degree would not be possible.

TABLE OF CONTENTS

LIST OF FIGURES

SEDIMENTATION BEHAVIOR OF ORGANIC - INORGANIC COMPOSITES BY OPTICAL TURBIDOMETRY

Reshma K. Harrinauth

ABSTRACT

Sedimentation is one of many characterization tools used to test materials in nanotechnology. Characterization of settling behavior is complex as there are many variables which can affect sedimentation. In our research, we focused on sedimentation in colloidal systems with the aid of an optical turbidometer. Nanoparticles of CeO_2 (Ceria Oxide) and TiO_2 (Titanium Dioxide) are embedded onto a polymeric matrix of a thermally responsive microgel of poly(N-isopropylacrylamide) (PNIPAM) and interpenetrating chains of poly(acrylic acid) to create novel composites. The composites are loaded with the inorganic oxide nanoparticles at different weight percent from a low value of 10 weight % to 75 weight %. The loading of the colloidal particles affects the sedimentation rate. In this thesis a turbidomenter is used to characterize the settling rate, which is an important characteristic for application of these new composites.

TiO_2 is a key constituent in many industrial products; cosmetics, paints, ceramics and used in waste water remediation. It is a potent photocatalyst which breaks down almost any organic compound when exposed to ultraviolet light. By combining nanoparticles of TiO_2 with microgels of a polymer, the composites can facilitate use and recovery of the catalyst. Gravity settling of these loaded composites provides an easy

separation of TiO_2 nanoparticles. In this context, characterization of settling plays an important role. CeO_2 composites are used to polish oxide coatings in the semiconductor industry and sedimentation of the composite particles is important as it can affect the efficiency of the planarization process. Therefore, measuring sedimentation of these composites is necessary.

In this study, the settling behavior is measured optically for a variety of conditions that differ in loading of inorganic nanoparticles within the microgels, temperature of the solution, and concentration of particles in solution. The overall goal is to understand the sedimentation behavior of these novel composites and facilitate their use in industrial processes.

NOMENCLATURE

A_f	Projected frontal area of the settling particle
C_D	Drag coefficient for a solid particle
d	Diameter of the particle
D_p	Diameter of the polymer
F_g	Gravitational force
F_b	Buoyant force
F_d	Drag force
g	Gravitational force
h_1	height from the top of the turbidometer holder to top of aperture
h_2	height from the top of turbidimeter holder to the bottom of the aperture
H	difference (h_2-h_1), representing the height of the window
I_o	Intensity of transmitted light
I_t	Intensity of incident light
L	Optical path length
N_p	number concentration of particles
N_{pi}	number of concentration of particle ‘i’
N_{Re}	Reynolds Number
t	Time
V_s	Settling velocity
$Y(V_{si})$	Fraction of total particles in class ‘i’

ρ_p Density of the polymer

ρ_f Density of the fluid

ρ_{sp} Bulk density of the settling particle

ρ_w Mass density of water

τ Turbidity parameter

τ_o Turbidity at initial time

υ Velocity of the object

μ Viscosity

μ_w Viscosity of water

CHAPTER ONE: INTRODUCTION

The main purpose of this thesis is to obtain a better understanding of novel composite particles by characterization of their sedimentation behavior. Sedimentation of particles has been utilized in fields ranging from engineering to wastewater remediation to materials science[1-5]. Sedimentation has also been the subject of many experimental and theoretical studies. In the latter case, development of a theoretical framework for sedimentation has been a challenge to many researchers when dealing with complex systems such as highly concentrated suspensions, polydisperse solutions, and aggregating or flocculating dispersions[6-8].

In this thesis, our interest lies in novel composite particles that combine organic polymers with inorganic metal oxides[9]. Composite materials are of increasing interest and are made up of two or more materials that are present together but remain chemically different entities. There has been a surge in research on composite materials as they are extremely useful in medicine, paints, and many cosmetic products[10-15].

Recently, novel composite materials that are composed of polymeric microgels and either titanium dioxide (TiO_2) or cerium oxide (CeO_2) nanoparticles have been developed[9]. Titanium dioxide is a widely recognized photocatalyst that has been used in wastewater remediation[10, 16, 17]. Nanoparticles of titanium dioxide, when exposed to ultraviolet light, have been found to be very efficient in the breakdown of organic matter. Cerium oxide nanoparticles are known to be useful in polishing silica wafers in the semi-conductor industry for planarization purposes[18-20].

Combination of these inorganic metal oxides within crosslinked and thermally responsive microgels (Figure 1.1) of poly (N-isoproprylacrylamide) provides many benefits for applications in photocatalysis or planarization. For example, embedding nanometer sized titanium dioxide particles within the polymeric gels can provide a useful method for the recovery and re-use of the TiO_2 photocatalyst. Cerium oxide nanoparticles embedded within the polymer microgels can eliminate surface scratches and defects for the case of chemical mechanical polishing since the composite particle has both soft and hard characteristics.

Sedimentation is known to be determined by density differences between the dispersed particles and the fluid medium as well as factors such as porosity when dealing with permeable systems. Therefore, measuring and interpreting settling behavior is a simple approach for characterizing composite particles. One goal of this thesis is to investigate the optical technique of turbidity measurement for characterization of the settling of composite particles and in turn, establish sedimentation as a tool for characterizing the ceria-microgel and the titania-microgel composite particles. A second goal is to explore the sedimentation behavior of titania-polymer particles as this can help in developing gravity settling approaches for separation and recovery of the photocatalyst. Finally, characterizing the settling behavior of the ceria-polymer particles is also important as it can affect the slurry polishing process.

The research performed in this thesis accomplishes the goals above. Chapter 2 of this thesis describes the technique of optical turbidity, the experimental apparatus, and the model for interpretation of the experimental data. Chapter 2 also reviews background information on optical turbidity and the validation of the technique against solid silica spheres using Stokes' Law. Chapter 3 describes settling of titanium dioxide composite particles and the effect of titania loading, temperature, and concentration on the sedimentation behavior. Here, optical

microscopy results are also presented to gain insight into the flocculation of the composite particles. Chapter 4 details the experiments on the ceria composite particles and the effect of temperature and loading on the settling behavior. Finally, Chapter 5 provides a summary and conclusions for the project.

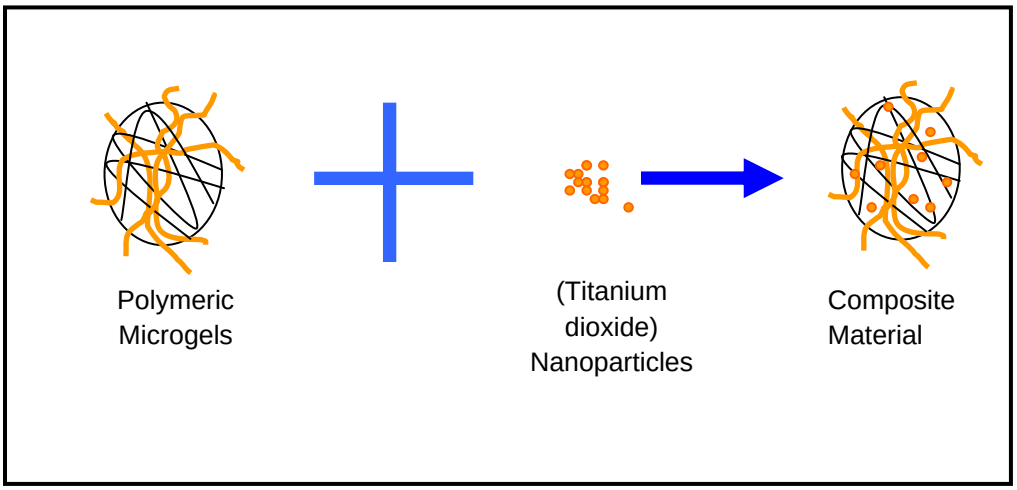

Figure 1.1: Schematic of the embedded nanoparticles within the polymeric matrix of a crosslinked microgel

CHAPTER TWO: TURBIDITY: MEASUREMENTS AND INTERPRETATION

2.1 Background

Optical techniques such as static light scattering, dynamic light scattering and turbidity measurements, due to their non-contact, non-invasive properties are well suited to the study of colloidal and macromolecular suspensions[21-26]. Static and dynamic light scattering are standard methods for investigating size, shape, and diffusion of particles and polymers in fluid media[27,28]. However, methods such as dynamic light scattering (DLS) are of limited use when characterizing systems containing particles that sediment since a necessary requirement for DLS is Brownian diffusion. Turbidometeric methods, on the other hand, have the advantage of being simple and well-suited to sedimenting systems.

Turbidity refers to light attenuation (by scattering and absorbing) from the presence of finely suspended materials[29, 30]. Turbidity measurements or nephelometry involve the relative measurement of intensity for light scattered through a range of angles and its ratio to the intensity of the incident beam. The use of nephelometry is a common procedure in environmental and water engineering where pollutant concentration or fine suspensions need to be routinely characterized[31]. The light attenuation by a single particle depends strongly on its size and for a collective suspension of particles, turbidity of the solution then becomes a function of both concentration of the particles and their sizes. Changes in the particle concentration due to sedimentation can be manifested in the turbidity of the solution. The goal in this chapter is to

demonstrate that measurement of the changes in turbidity of a solution with time provides a simple and convenient method to characterize colloidal suspensions.

2.2 Experimental apparatus

The experimental apparatus used to measure the settling rate of the particles was a turbidometer (model DRT 1000, HF instruments). The turbidometer works in a simple manner wherein light is scattered at a 90^o angle to the incident beam and a photo detector converts the light intensity into a voltage[29]. A schematic of the turbidometer is seen in figure 2.1. As shown in the figure, a standard size cylindrical test tube (12mm x 75 mm) contains the particle solution. A water bath was connected to the turbidometer holder to circulate water and maintain a desired temperature. The photodetector signal was recorded using a computer with a program written in Hewlett Packard Visual Engineering Environment (HP VEE). During the experiment, 1000 points were acquired at an analog-to-digital sampling frequency of 1 kHz and the mean value of the voltage was recorded as a function of time. For samples which took much longer than a day for settling, a timer was used to switch the turbidometer on and off.

2.3 Sedimentation and Stokes Law

Sedimentation, where particles fall under the action of gravity through a fluid in which they are suspended, is a way of separating particles from fluids as well as classifying particles with different settling speeds[1]. Stokes law has been commonly used to predict the velocity of a single solid particle in an infinite fluid medium at low Reynolds number[1, 4, 32]. A particle settling in a liquid is acted upon by the gravitational force, buoyancy force, and the fluid drag force. As indicated by the figure 2.2, the gravitational force, F_g, acting in the downward direction is

counteracted by the buoyancy force and the drag force. The terminal velocity of the particle is achieved when drag force is equal to the gravitational force minus the buoyancy force

$$F_g - F_b = F_d \qquad (1)$$

The net gravitational force on a sphere can be given as[33]

$$F_g - F_b = \pi\left(\rho_p - \rho_f\right)g\frac{d^3}{6} \qquad (2)$$

The drag force can be further written as:

$$F_d = \frac{1}{2}C_D A_f \rho_f \upsilon^2 \qquad (3)$$

The drag coefficient (C_D) is a function of several parameters, such as particle shape, particle aggregation, permeability, and fluid characteristics [33]. For creeping flow or Stokes regime, where the inertial effects are negligible, the drag coefficient for a spherical solid particle can be given exactly as[33-35]:

$$C_d = \frac{24}{N_{\mathrm{Re}}} \qquad (4)$$

where N_{Re} is the Reynolds' number and can be expressed as:

$$N_{\mathrm{Re}} = \frac{\rho D_p V_s}{\mu} \qquad (5)$$

Thus, the Stokes settling velocity for solid spherical particles is as follows[9, 33-35]

$$V_s = \frac{\left(\rho_{sp} - \rho_w\right)g}{18\mu_w}D_p^2 \qquad (6)$$

Settling behavior under Stokes' law is valid for very dilute suspensions, where hindered settling effects are negligible, and for either a small solid spherical particle or a very viscous medium (N_{Re}<<<1).

One of the first tasks in our research was to validate the use of turbidity measurement to measure settling velocity. Towards this end, we measured settling of solid silica spheres of two different sizes and compared the results with the prediction of Stokes' law.

2.4 Interpretation of turbidity during sedimentation

The established theory of photo-sedimentation uses low volume fraction of particles and measures the attenuation of the light beam occurring by the particles at varying settling depths as a function of time[31]. The attenuation can be expressed as $\left(\frac{I_t}{I_o}\right)$ and a single turbidity parameter is commonly used, (τ), which is the fractional decrease in intensity of light. The turbidity can be simply related to the number of particles per unit volume (N_p) by

$$\tau = \frac{1}{L}\ln\left(\frac{I_o}{I_t}\right) \;\alpha\; N_p \qquad (7)$$

Equation (7) suggests that a normalized turbidity signal can provide information on the evolution of particle concentration due to sedimentation[36]. For particles with a single settling V_s, we can use the following equation for the turbidometer setup shown in figure 2 with H being the height of the aperture (h_2-h_1)[36]:

$$\frac{N_P(t,V_s)}{N_p(0,V_s)} = 1 - \frac{V_s}{H}\left(t - \frac{h_1}{V_s}\right) \qquad (8)$$

In figure 2.3, the schematic shows the concentration of the particles settling in the test tube with a single velocity. At a time t_1, the particles fall through a height of h_1 and the normalized turbidity signal starts decreasing because the concentration in the optical aperture starts to decrease. As the particles continue to fall with the same rate, a linear decay in the signal is observed as shown in the graph. Once the majority of the particles have fallen through the region where the light enters (between h_1 and h_2), the turbidity signal goes to zero.

In the case of the composite particles, different settling velocities would be observed due to differences in loading of the nanoparticles. In this case, it has been shown by Coutinho and coworkers that the evolution in the normalized turbidity signal can give a distribution of settling velocities by using the following relation[36].

$$\frac{\tau(t)}{\tau_o} = \Sigma\left(\frac{N_{pi}(t, V_{si})}{N_{pi}(0, V_{si})}\right) Y(V_{si}) \qquad (9)$$

In this equation, the number of particles in class, *'i'* at intial time, is indicated by N_{pi} (0, V_{si}) where the settling velocity is V_{si}. The number of particles in class *'i'* with a settling velocity of V_{si} at time *t* in the sampling window is then N_{pi} (t,V_{si}) and Y(V_{si}) is the fraction of total particles in class *'i'*. Complete details of the mathematical model are available in the paper by Coutinho, Harrinauth, and Gupta[36].

2.5 Results and discussion

Solid silica spherical particles were used to validate the experimental method and the mathematical model. Commercially available, 'large' silica sphere particles with an average diameter ~3.21±0.35μm were suspended in deionized water and turbidity measurements were

performed. Figure 2.3 shows settling data for the large silica spheres. We can make an easy estimate of the settling velocity using equation 8 from the value of t_1, which is the time at which the turbidity signal starts to drop steeply in figure 2.3. The experimental data indicates that t_1~7500 seconds. Using the value of h_1=3.9 cm (Figure 2.1) of the turbidometer, we can estimate that the average settling velocity is ~5.2×10^{-4} cm/s. Applying Stokes' law with the known properties of the particle and the fluid, the settling velocity can be predicted to be 5.4×10^{-4} cm/s, which clearly indicates good agreement between the settling measured using the turbidity setup and theoretical expectations. A more accurate analysis of the turbidity signal that captures the small variations in terms of polydispersity effects can be performed using equation 9. Coutinho and coworkers have shown that this analysis allows interpretation of the turbidity signal as a distribution of settling velocities[36].

In addition to the large silica particles, settling behavior of fine silica particles was also performed. These fine silica particles were synthesized in the research laboratory using a sol-gel technique (materials courtesy of Shim and Gupta) and had a diameter of ~450±30nm. Figure 2.4 shows the data for settling of these sub-micron particles. The impact of the small size is easily observed by the long settling times. The complete settling occurred over five days. Figure 3.4 also indicates that in the case of these small particles it is more difficult to distinguish a sharp break in the turbidity signal. As a quick estimate we can pick a time where the most noticeable change in slope is occurring and this gives t_1=2.5 days. Using a similar reasoning as before, the estimated average settling velocity is then 1.8×10^{-5} cm/s. The settling velocity of the fine particles calculated via Stokes' Law is 1.1×10^{-5} cm/s, which is in good agreement with the estimate from experiments. In the case of the fine particles, the more accurate analysis of the settling distribution has been performed by Coutinho and coworkers[36], which shows that the

velocity distribution is broader than the case for the large particles and is consistent with the absence of a sharp break in the turbidity signal.

In summary, the turbidity measurements for the solid silica spheres across a size range of approximately 0.5 – 5μm agree very well with the expected results from theoretical relation such as Stokes law. This provides support for the potential use of turbidity measurements as a simple and useful tool to characterize composite particles by analysis of their sedimentation behavior. The following chapters focus on the characterization two novel composite particles made from titania nanoparticles in a polymeric microgel and ceria nanoparticles in a polymeric microgel.

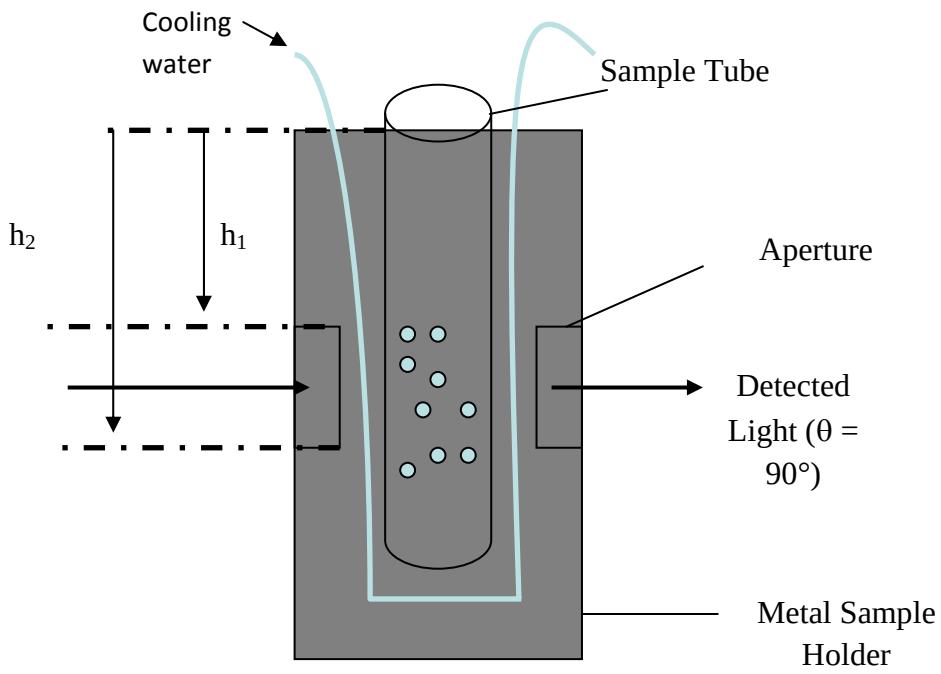

Figure 2.1 Schematic of turbidometer set-up for settling experiments

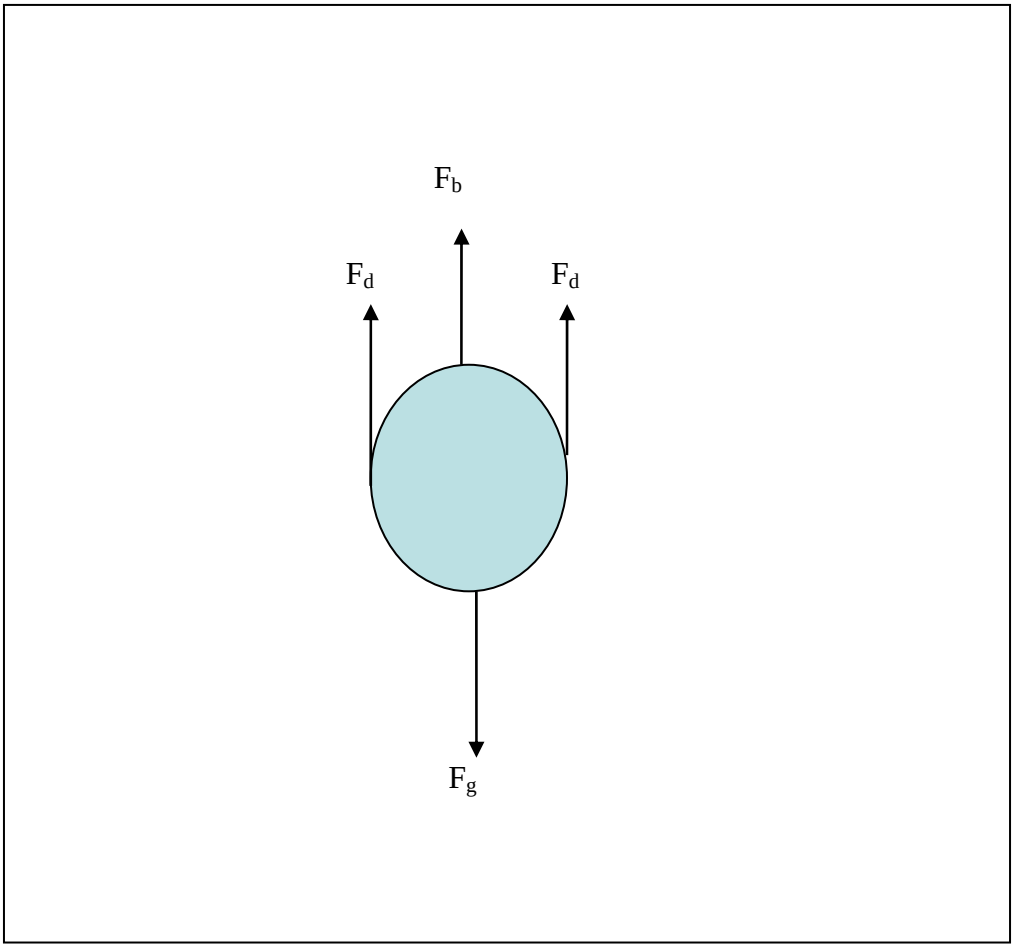

Figure 2.2 Schematic of forces acting on a particle settling in liquid

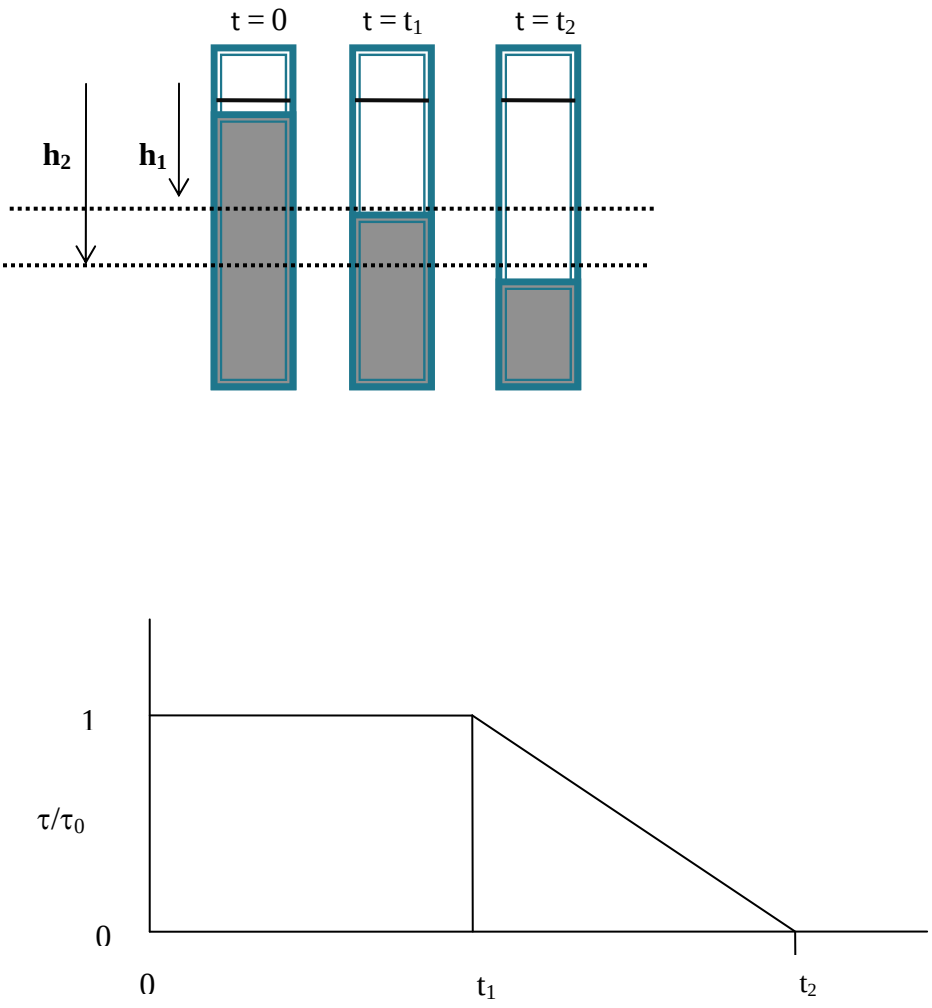

Figure 2.3 Schematic of normalized turbidity

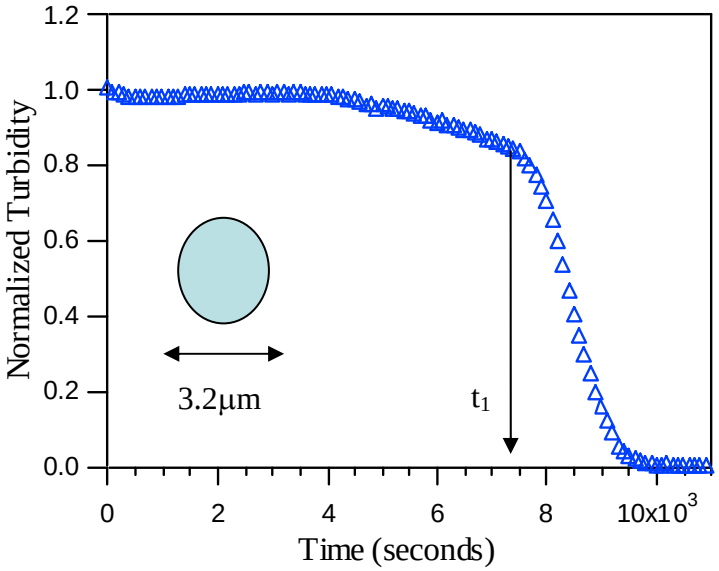

Figure 2.4 Normalized turbidity signal for the settling ‘large’ silica spheres

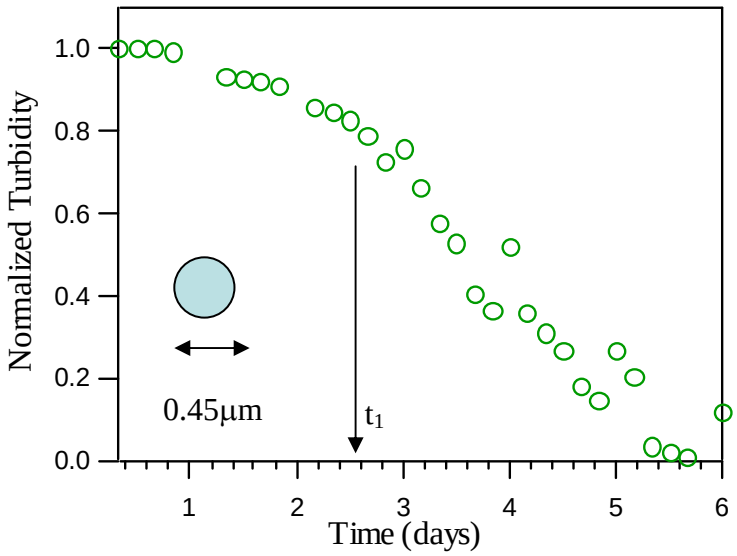

Figure 2.5 Normalized turbidity signal for the settling ‘fine’ silica sphere

CHAPTER THREE: SETTLING OF TITANIUM OXIDE COMPOSITE

3.1 Introduction

Titanium dioxide (TiO_2) is a common metal oxide that has emerged as an excellent photocatalyst material in environmental remediation[37, 38]. Titanium (IV) oxide exists in nature in two tetragonal forms as rutile and anatase. A third form, Brookite, is a rhombic form. Anatase and rutile can be easily prepared in the laboratory and these two forms have been used in many photocatalytic studies[39]. Commercially available TiO_2 is commonly Degussa™ P25, which contains the anatase and rutile phases in a ratio of about 3:1[7].

Photocatalytic reaction on TiO_2 surfaces has generated a great deal of interest in chemical degradation of contaminants because of its low cost, simplicity, and high efficiency[10, 34, 37, 40]. Organic chemicals that are found as pollutants in wastewater from industrial or domestic sources must be removed or destroyed before being released to the environment. These pollutants can also be found in ground and surface waters, which also require treatment to achieve potable quality. The increase in these environmental pollutants has seen a rise in public concern for the development of novel treatment methods. Using nano-scale TiO_2 greatly increases the surface area of titanium dioxide and permits a better reduction of organic pollutants in wastewater remediation.

However, the recovery of titania nanoparticles suspended in an aqueous medium has remained a challenge. In this context, the attachment of TiO_2 nanoparticles to polymeric microgels is an innovative approach to address recovery and use of TiO_2 photocatalyst. Coutinho

and Gupta have shown that cross-linked microgels of PNIPAM containing interpenetrating chains of poly(acrylic acid) (PAAc) allow composite particles to be prepared that can settle rapidly[36]. The titania retains its chemical identity and works as an excellent photocatalyst while the highly porous microgel allows light to reach the nanoparticle surface and permits easy exchange of fluid. The rapid settling of the composite facilitates the retrieval of the composite material in an efficient manner. In this chapter, the settling of titanium dioxide composite particles, the effect of titania loading, temperature, and concentration is evaluated.

3.2 Experimental method

Different stock solutions of the titania-microgel composite containing a fixed, average mass fraction of titania (10%-75%) were used. Prior to characterization in the turbidometer, each stock solution was diluted with the addition of deionized water to a total volume of $5cm^3$. To study the effect of particle concentration, the relative amounts of stock solution and water was varied. The test tube with the sample solution was sealed from the top with Parafilm™ and sonicated for 5 minutes to redisperse the particles uniformly in solution. The sample was then removed and placed in the turbidometer holder for approximately five minutes to ensure the content is equilibrated at the desired temperature. After thermal equilibration, the sample was then quickly removed and inverted four times in order to redisperse the particles.

Acquisition of the turbidity as a photodetector voltage was performed every five seconds as described in Chapter 2. Eight runs were performed for each sample and these were averaged. In the experiments that were conducted at 15°C, the test tube had to be wiped after each run with kimwipe as a thin layer of condensation was formed on the outside of the test tube. It should be

noted neither the polymeric microgels without any titania nor the titania nanoparticles alone settle over a time frame of days.

Flocculation of the composite particles was also examined using optical microscopy of flocs deposited on a glass slide. Since the flocs were very small, in order to measure the area of the flocs it was very important that the glass slide was cleaned properly of any dust particles. The glass slide was cleaned thoroughly by initially soaking it in deionized water. The glass slide was then carefully removed from the water bath and placed into a soapy water bath solution. A second clean water bath was used to rinse the soap and the glass slide was then dried with the aid of a stream of nitrogen.

Each loading of the titania composite was measured using optical microscopy. A test tube containing 850μl of the titania-composite stock solution and 4.15ml of water was shaken and agitated in the same manner as the turbidity testing. The clean glass slide was placed into a large Petri dish and the content of the test tube was poured gently onto the glass slide and the settled aggregates on the slide were observed in transmission using an optical microscope. Objective lenses with 4X and 10X magnification were used in order to view the flocs.

3.3 Results and discussions

3.3.1 Effect of titania loading

Understanding settling of the titania-microgel for different loadings of titania nanoparticles is an important aspect of this research. The settling rate of the composite particles will be an important piece of information in any process application where gravity settling of the composites will be exploited.

In this study, particles with various weight percentages of titania nanoparticles ranging from 10% to 75% have been characterized. As the mass fraction of the titania increases, the effective density of the particle increases and this should also impact the sedimentation of the particles. We can calculate the effective density of the dry polymer particles as

$$\rho_p(f) = \frac{\rho_{pol}\rho_{TiO_2}}{(1-f)\rho_{TiO_2} + f * \rho_{pol}} \qquad (10)$$

where ρ_{TiO2} is the density of the TiO_2 (~ 4.16 g/cm^3), f is the mass fraction of the TiO_2 per particle, ρ_{pol} is the density of the polymer (~1.07g/ml)[9]. From the equation given above, 10% of titania loading in each particle gives the effective density of the composite as 1.16 g/cm^3. At 75% loading of the titania particles, the effective density changes to 2.42 g/cm^3. Thus, there is a substantial change in effective density of the composite particles with increase in its titania loading.

Figure 3.1 shows the settling data as normalized turbidity for the various loadings of titania in composite particles at ambient temperature (~25°C). It is clear from the data, that at the lowest loading of 10% the settling is slowest and at the highest loading of ~75%, the settling is fastest. The data in figure 3.1 shows that when f=10%, the settling time is approximately 2000 seconds. For values of loading of 25% and 50% loaded, the particles show a settling time of approximately 300 seconds and 600 seconds. In contrast, particles with 75% titania settle extremely rapidly in approximately 100 seconds.

Coutinho and coworkers[9] have shown that the mean settling velocity of the composite particles obtained from data in figure 3.1 can be correlated to the average loading of titania. A theoretical framework that accounts for both the changes in effective density and the changes in

permeability of the particle with increased loading of titania has been applied by Coutinho and coworkers. Thus, results such as those shown in figure 3.1 clearly indicate the usefulness of turbidity measurements for characterizing the novel composite particles as the measurement of settling velocity can be rapidly interpreted in terms of average loading of the titania photocatalyst in the composites.

3.3.2 Effect of temperature

One of the polymeric constituents in the composite particles is PNIPAM, which is a thermally responsive polymer and is known to exhibit a lower critical solution temperature(LCST) near 32°C in aqueous solutions[41, 42]. Stimuli responsive polymers, where the polymer can change size in response to external stimuli like temperature, pH and ionic strength, have many applications[36, 41]. For cross-linked polymeric microgels of PNIPAM, when the solution temperature is low, the polymeric microgels absorb water and exhibit a swollen state. At high temperatures, an abrupt volume shrinkage of the particle results in expulsion of free water within the polymer network[42-48]. The expansion and collapsing property of PNIPAM microgels has been extensively investigated in the field of drug delivery system, biosensors, tissue engineering[42-47].

Figure 3.2 shows schematically the swelling and shrinking of the polymeric microgels at a transition temperature. The microgels used in this study were approximately 750nm in the swollen state and 330nm in the collapsed state. As mentioned earlier, chains of a polyelectrolyte (PAAc) were were introduced within the cross-linked PNIPAM microgel to promote the loading of the TiO_2 nanoparticles within the polymeric particles[36]. The change in the overall volume of the microgel as it transitions with temperature can affect the effective density of the composite particle and also the permeability, which are both important factors in the settling behavior.

Figure 3.3 shows the settling behavior of composites containing 25% by weight of titania at three temperatures. The experimental data shows that as the temperature increases from 15°C to 25°C, the composite particles settle at earlier times. Further increase beyond the transition temperature has a significantly smaller effect. We can qualitatively understand this trend in terms of the changes in the particle properties. At the low temperature of 15°C the particle is highly swollen with water and has a very high porosity (> 0.95). As a consequence, the effective density contrast between the particle and water is very low, which makes the particle settle slowly. As the temperature increases, there is a decrease in the size of the polymer microgel due to the thermally responsive nature of the PNIPAM. The increase in density due to smaller size appears to dominate the effects of porosity and the particle settles faster.

Figure 3.4 shows the experimental data on settling for a composite with 50% titania loading at the three temperatures. The general effect of temperature here is similar to the 25% loading. However, the shift in settling between 15°C and 25°C is perceptibly smaller because the particles were denser to begin with and settled faster.

3.3.3 Effect of concentration

Concentration of the sample is an important characteristic of the settling behavior as the particle to particle interaction is an important contribution. It is known that for solid particles as the concentration of the sample becomes too high, hindered settling can occur and reduce the settling velocity. Therefore, the effect of concentration was studied to ensure that all the experiments did not entail hindered settling.

Figure 3.5 shows data for three different dilute concentrations of the sample particles. Over the range of particle concentrations studied, it is clear that even a four-fold increase in

particle mass concentration (0.083 mg/ml to 0.33 mg/ml) does not change settling time significantly (the change of a few tens of seconds is within the error of the measurement). We can conclude that the particle concentration in all our experiments is low enough that effects of hindered settling can be discounted.

3.3.4 Optical microscopy of flocculated composite particles

Smoluchowski was one the first scientists to examine the dynamics of floc growth for suspensions subjected to shear and showed that collision of the fine particles with interactions could lead to an increase in the size of the aggregates[49]. Since the titania-microgel composite particles have polymeric chains of PAAc that can interact with other particles through the PAAc chains as well as titania nanopartiles in the neighboring particles, we have observed that these composites have a tendency to aggregate as they settle within the sample test tube.

Coutinho and coworkers[9] have shown the floc formation and the ensuing increase in size as well as porosity are very important in the low drag force and rapid settling of the composite particles. In the settling tube, the appearance of the flocs is very powdery. These flocs are also very delicate and under slight agitation break apart very easily. To gain some insight into the nature and sizes of these aggregates, analysis of the flocs was done using optical microscopy.

Figures 3.6 to 3.9 show optical images of the flocs formed using composites with two different loading of titania. As shown in the figures we can observe the range of the aggregates size. Regardless of the loading of the oxide, the sizes of these aggregates were within 10-100 μm and their appearance is very similar. Coutinho and coworkers[9] have shown that by accounting for the fractal-like nature of these flocs and by modeling the settling of these highly porous, large aggregates can explain the rapid settling of the composite particles. They have

found that good agreement between theoretical predictions and experimental data can be found when the floc size of 10-100 μm is used.

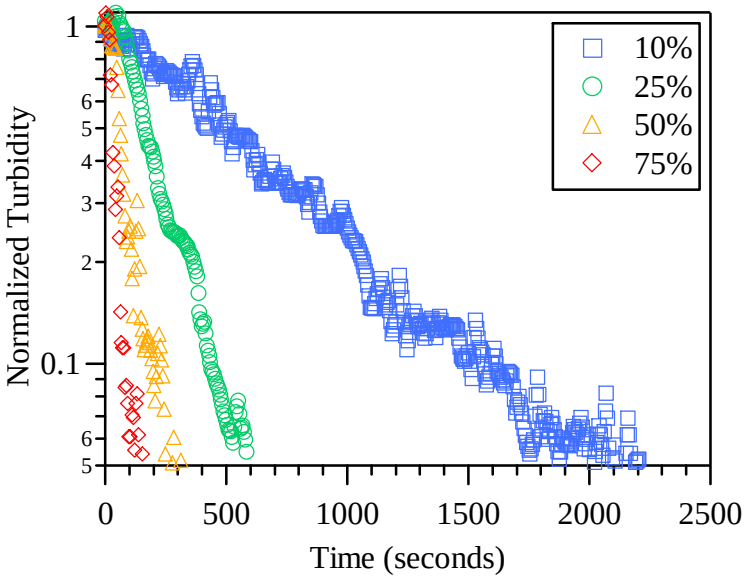

Figure 3.1: Settling of composites at various weight percentage of titania in each particle

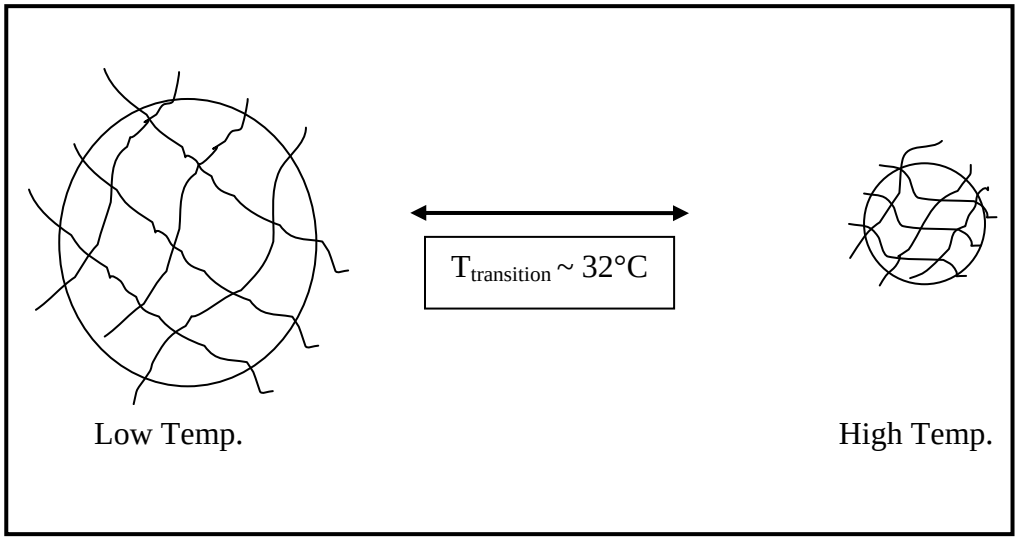

Figure 3.2 Schematic of microgel response above and below the volume phase transition temperature.

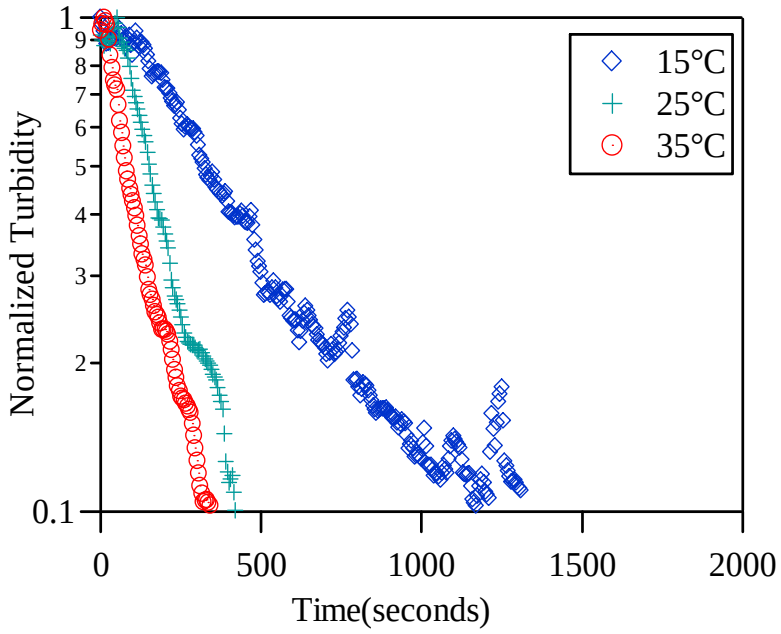

Figure 3.3 Settling of composite with 25% titania at temperatures below and above transition temperature (T~32°C)

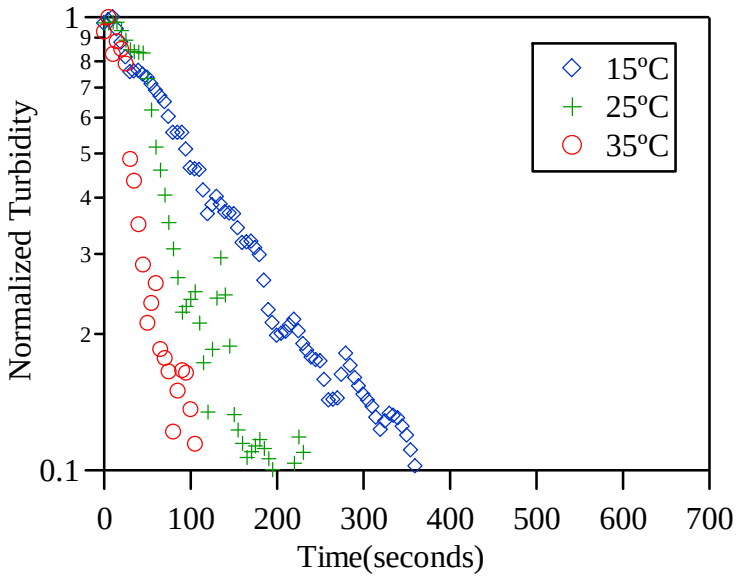

Figure 3.4 Settling of composite with 50% titania at temperatures below and above transition temperature (T~32°C)

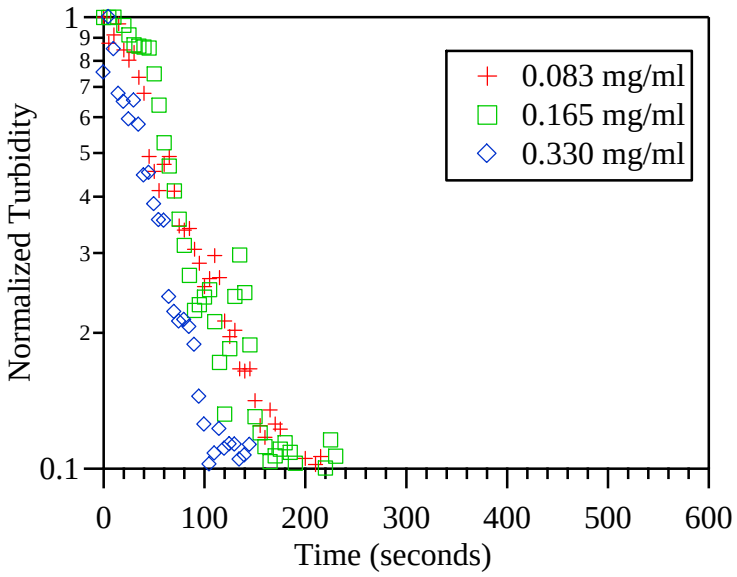

Figure 3.5: Settling of composite with 50% titania and different particle concentration in solution

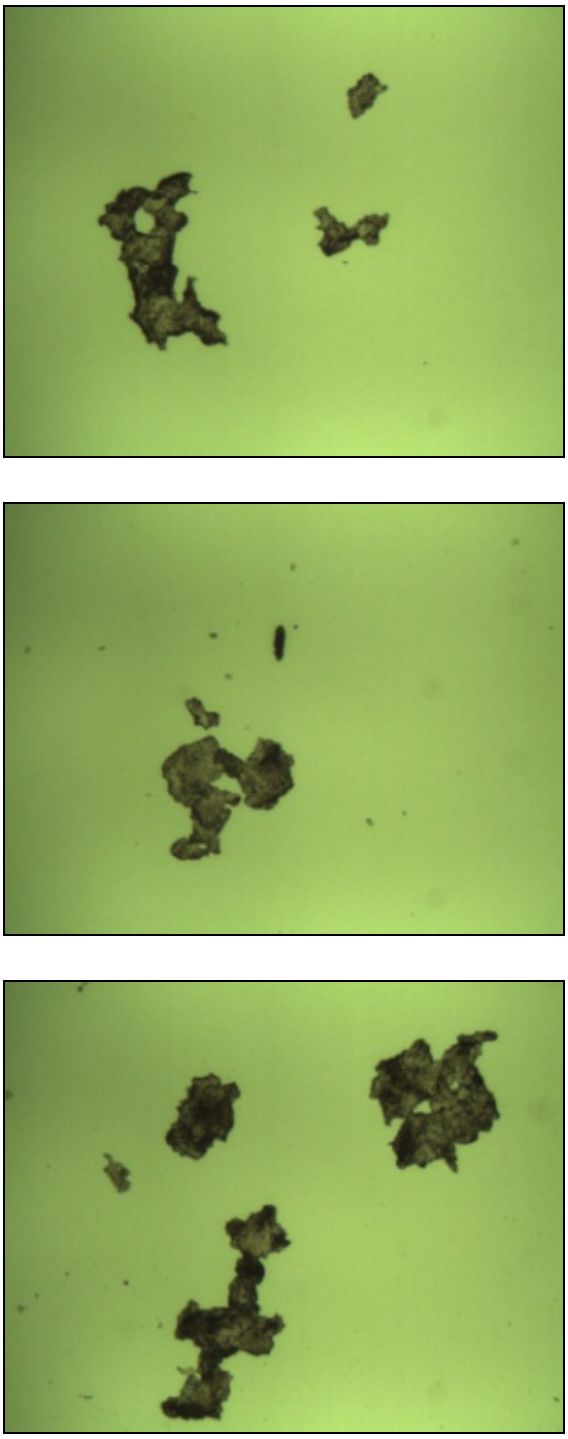

Figure 3.6 Optical images of flocs of composites with 50% titania at 4X magnification. The image size is 2672μm x 2136 μm.

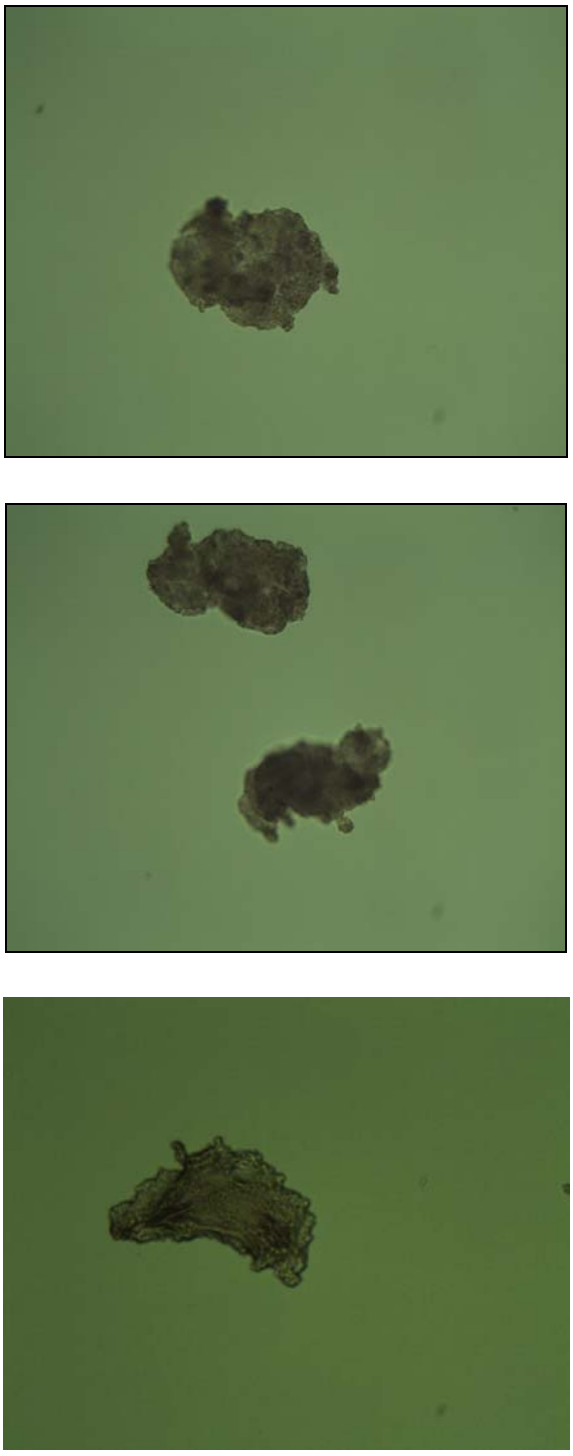

Figure 3.7 Optical images of flocs of composites with 50% titania at 10X magnification. The image size is 1069 μm x 854 μm.

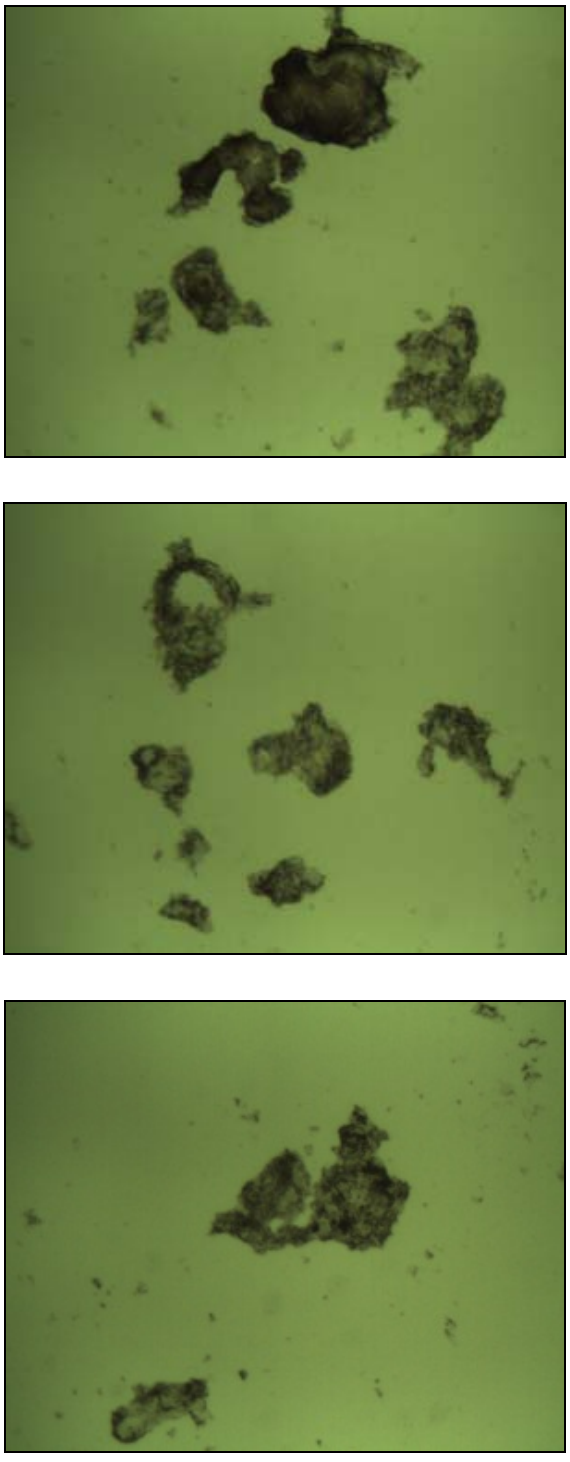

Figure 3.8 Optical images of flocs of composites with 75% titania at 4X magnification. The image size is 2672 μm x 2136μm.

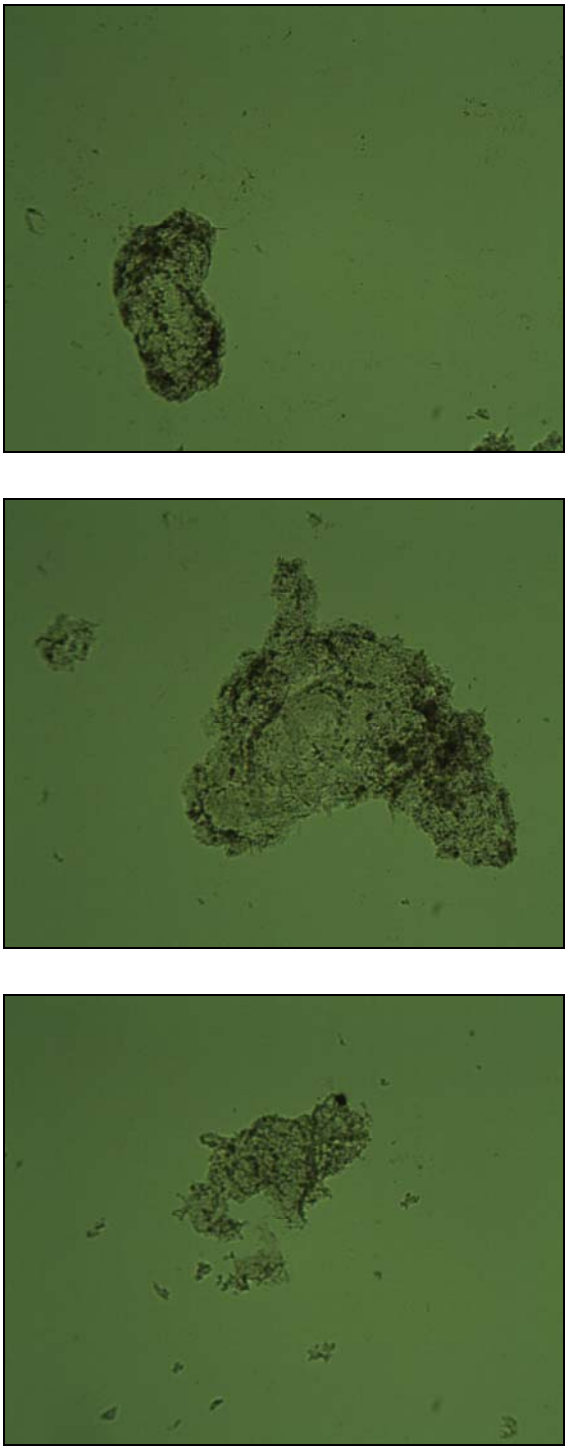

Figure 3.9 Optical images of flocs of composites with 75% titania at 10X magnification. The image size is 1069 μm x 854 μm.

CHAPTER FOUR: SETTLING OF CERIUM OXIDE COMPOSITE

4.1 Introduction

The rapid advances in the microelectronics industry demand significant improvements in Chemical Mechanical Polishing (CMP), which is a widely used technique for the planarization of metal and dielectric films to accomplish multilevel metallization (Figure 4.1). As the microelectronic device dimensions keep on decreasing and the minimum feature size becomes smaller than 0.1 μm, a very thin layer of material has to be removed and a flat and clean surface finish has to be achieved during the polishing of wafers. The fabrication of these small devices without imperfections requires improvements in the CMP process[19, 50, 51].

The CMP process generally consists of a rotating wafer pressed face down onto a rotating, resilient polishing pad while polishing slurry containing abrasive particles and chemical reagents flows in between the wafer and the pad. A schematic of the CMP process is illustrated in figure 4.1. The combined action of polishing pad, abrasive particles and chemical reagents results in material removal and polishing of the wafer surface[52]. The polishing slurry provides both chemical and mechanical action where it is used to remove and planarize the wafer surface. The mechanical action helps achieve the required planarization and uniformity of the silica wafer which is accomplished by the use of the abrasive particles in the slurry. The chemical action is achieved by the slurry incorporating oxidizing agents or additives content which improves degradation. The erosive action in CMP is mostly provided by the submicrometer size abrasive

particles as they flow between the pad and wafer surface under pressure. The magnitude of the mechanical action is in turn determined by the size and nature of the abrasive particles. The major process variables in CMP are the platen speed, down force and the slurry[18, 19, 50, 51].

The use of hard inorganic particles in commercially available slurries can cause scratches on the surface of the wafer. It has been studied in the past that mixed or modified abrasive particles can reduce the number of imperfections on the wafer[53, 54]. The creation of a novel inorganic- organic composite particle of the types discussed in earlier chapters has been proposed as a good candidate to be used as an abrasive slurry in the CMP process[55, 56]. In these novel particles, the polymeric network consists once again of the PNIPAM microgels and interpenetrating chains of PAAc. In addition, siloxane functional group was incorporated onto the network. Ceria nanoparticles have been shown[19, 20] to be useful in CMP and therefore, these new composites are ceria-microgel rather than titania-microgel. The characteristics of the composite particle are the softness of the polymer network and surface hardness due to the presence of the ceria nanoparticles. This combination allows for the use of the composite particle to be suitable for the prevention of defects and any aggressive scratching on the wafer. One of the main characteristic behaviors of the ceria loaded composite particles is the settling rate, which is an important parameter during the slurry polishing. Therefore, in this chapter the sedimentation behavior of the ceria-polymer composites has been explored as a function of temperature and loading. As a comparison, the sedimentation of ceria nanoparticles alone is also characterized.

The experimental set-up for the settling studies was similar to the titania-microgel particles and has been described in Chapters 2 and 3. Briefly, the ceria composite was added to the turbidometer sample tube from the stock solution and diluted with deionized water. The

sample was placed in the turbidometer and where it was allowed to equilibrate to the desired temperature. It was quickly removed and inverted to ensure the particles were fully dispersed in the suspension. It was placed into the turbidometer holding and data was acquired using the data acquisition software as described in section 2.2

4.2 Result and discussion

The use of pure ceria particles was used as a reference for the settling time for the hybrid ceria particles and it is observed in figure 4.2 that these nanoparticles settle over a long time of approximately 12000 seconds. Figure 4.2 also shows the settling of the polymer composites loaded with 50% and 25% ceria nanoparticles. The loading of the particles affects the sedimentation rate and similar behavior to the titania microgels was observed. At the 50% loading there is a faster settling time of approximately 1500 seconds at ambient temperature (25°C). This faster settling time indicates that the effective density of the hybrid particles has increased substantially from the bare ceria nanoparticles. The 25% loaded ceria composite had a settling time of 3500 seconds and again this is a substantial difference in the sedimentation rate of the pure ceria particles. The trend with ceria loading is similar to that for the titania-microgel composites where decreasing the loading caused slower settling.

The effect of temperature also had an effect of the settling rate of the 25% and 50% ceria–microgels. In figure 4.3 the temperature at 35°C shows a settling time of approximately 1000 seconds for the 50% ceria-microgel composites. However as the temperature decreases to 15°C the settling rate is longer, the particle settles at approximately 1800 seconds. The 25% ceria loaded particles were also tested at temperatures of 25°C and 35°C (Figure 4.4). The settling time was 4000 seconds and 2000 seconds, respectively. As discussed in Chapter 3, the changes

in temperature affect the porosity of the particles, their size, and the density contrast with the fluid. The results in Figure 4.3 and 4.4 show that as the temperature of the composite particle suspension decreases below the transition temperature, the drag force decreases. The results also show that when using the hybrid ceria composite particles, the enhanced settling of the particles in the slurry will require continuous agitation of the slurry mixture to maintain uniform particle distribution.

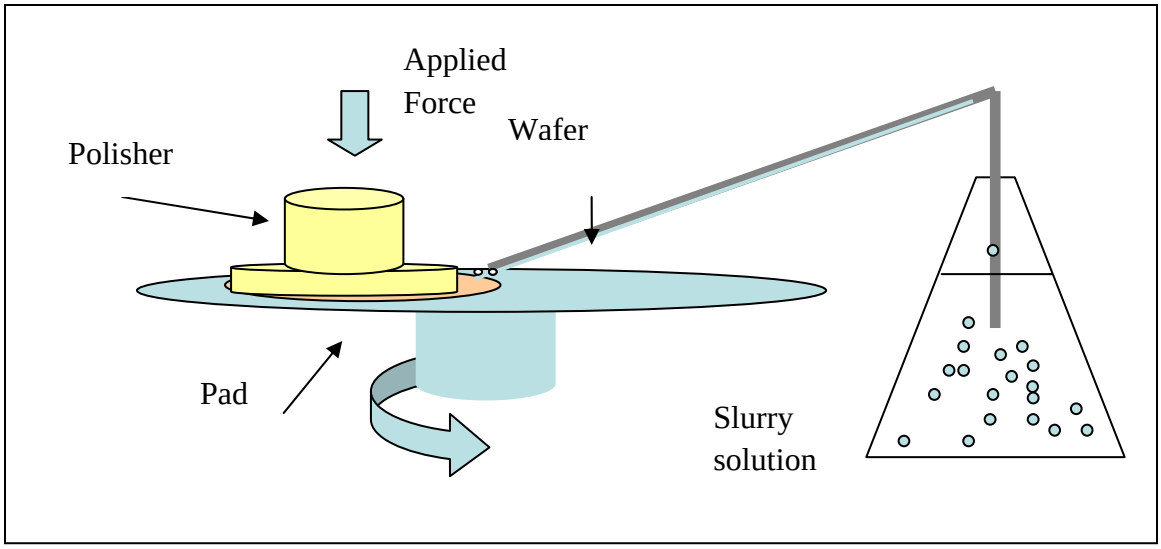

Figure 4.1 Schematic of slurry polishing in a CMP process.

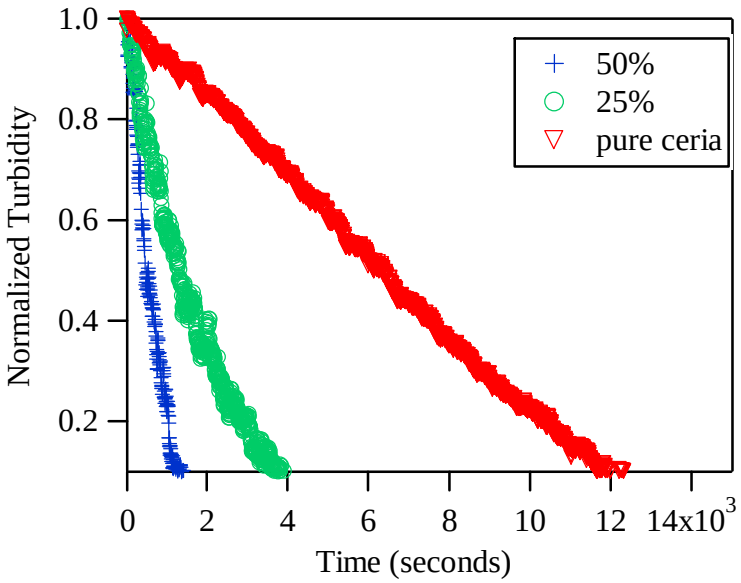

Figure 4.2 Settling of pure ceria nanoparticles at ambient temperature compared against composites with 25% and 50% ceria loading.

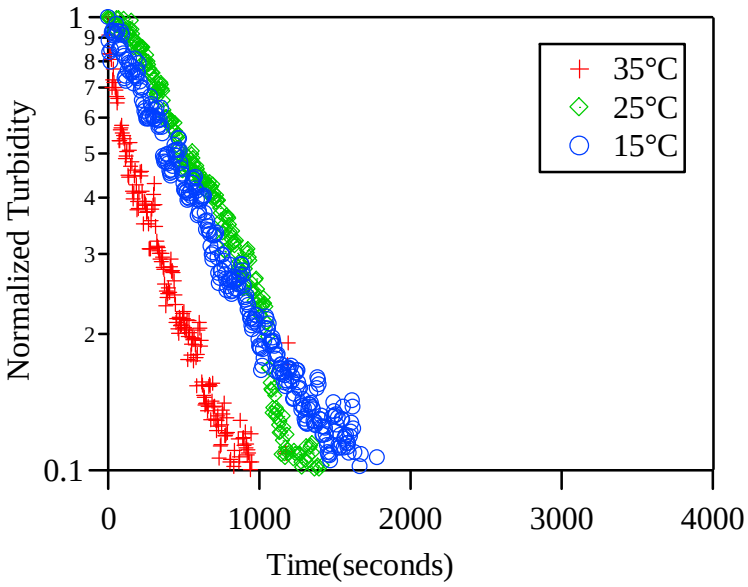

Figure 4.3: Settling of composite with 50% ceria at temperatures below and above the transition temperature (T~32°C)

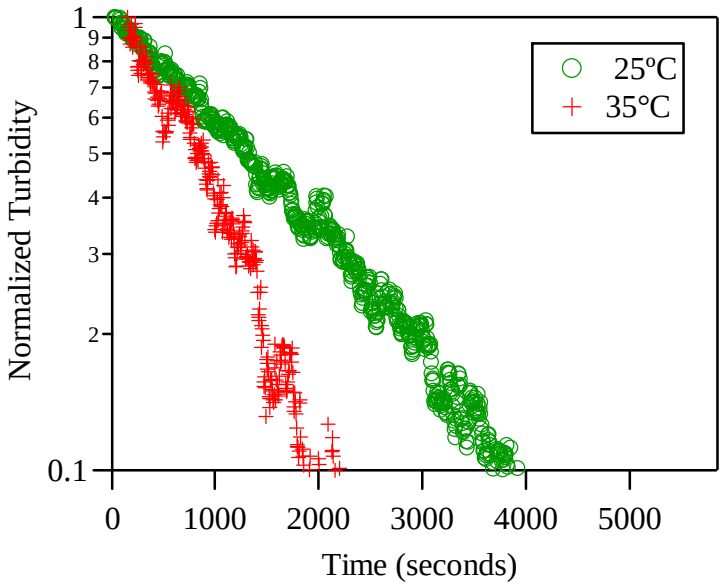

Figure 4.4: Settling of composite with 25% ceria at temperatures below and above the transition temperature (T~32°C)

CHAPTER FIVE: SUMMARY AND CONCLUSIONS

In summary, this thesis has focused on the sedimentation of two composite particles with an interpenetrating network of polymers and embedded with inorganic oxide nanoparticles of titania or ceria. The focus has been on the characterization of these particles via sedimentation. Turbidity has been used as a simple technique to identify the settling rate of these colloidal particles. The settling rate of solid silica particles has been used to validate the technique by comparing theoretical predictions of settling with the experimental method.

The novel titania-microgel particles have shown rapid settling behavior once the titania nanoparticles are embedded within the polymeric framework. This has been advantageous in the field of waste water remediation where the titania nanoparticles are used as photocatalyst and the recovery of the composite particles can be much simpler using sedimentation. It was found that the loading of the titania nanoparticles onto the framework of the polymeric network effectively changes the density of the particles and the increased porosity of the flocs of the composites affects the settling rate of these particles. Temperature is also a factor since the polymeric framework consists of a temperature sensitive polymer, PNIPAM, which causes the particles to exhibit a collapse and expansion behavior near a transition temperature. The combined influence of changes in effective density and the porosity with temperature influence the settling behavior.

The use of novel composite particles with embedded ceria nanoparticles is effective in the CMP process and these can be used as an alternative for the commonly used commercial

abrasives. However, the ceria-microgels show rapid settling rates and indicate that constant agitation is required for their suspension.

Overall, the technique of sedimentation is ideal in the case of characterizing these composite particles as it forms the basis of a simple characterization. The experiments in this thesis have explored the settling rate of porous composite particles and shown that a variety of parameters such as temperature, particle loading, and concentration affect the settling behavior. Combination of experiments such as the ones described in this thesis with theoretical understanding can be valuable in the study of complex systems of polymeric microgels and inorganic nanoparticles.

REFERENCES

1. Johnson, C. P.; Li, X.; Logan, B. E., Settling Velocities of Fractal Aggregates. Environmental Science and Technology 1996, 30, (6), 1911-18.

2. Shojaei, A.; Arefinia, R., Analysis of the sedimentation process in reactive polymeric suspensions. Chemical Engineering Science 2006, 61, (23), 7565-7578.

3. Je, C.-H.; Chang, S., Simple approach to estimate flocculent settling velocity in a dilute suspension. Environmental Geology (Berlin, Germany) 2004, 45, (7), 1002-1009.

4. Kulkarni, P.; Dutari, G.; Biswas, P.; Haught, R., Gravity settling characteristics of Cryptosporidium parvum oocysts in aqueous suspension using in situ static light scattering. Colloids and Surfaces, A: Physicochemical and Engineering Aspects 2004, 233, (1-3), 1-10.

5. Dai, X.; Boll, J., Settling velocity of Cryptosporidium parvum and Giardia lamblia. Water Research 2006, 40, (6), 1321-1325.

6. Franks, G. V.; Sepulveda, C. V.; Jameson, G. J., pH-sensitive flocculation: settling rates and sediment densities. AIChE Journal 2006, 52, (8), 2774-2782.

7. Davies, R., The experimental study of the differential settling of particles in suspension at high concentrations. Powder Technology 1968, 2, (1), 43-51.

8. Bürger, R.; Concha, F.; Fjelde, K. K.; Karlsen, K. H., Numerical simulation of the settling of polydisperse suspensions of spheres. Powder Technology 2000, 113, (1-2), 30-54.

9. Coutinho, C. A.; Harrinauth, R. K.; Gupta, V. K., Settling characteristics of composites of PNIPAM microgels and TiO2 nanoparticles. Colloids and Surfaces A: Physicochemical and Engineering Aspects 2008, 318, (1-3), 111-121.

10. Fujishima, A.; Rao, T. N.; Tryk, D. A., Titanium dioxide photocatalysis. Journal of Photochemistry and Photobiology C: Photochemistry Reviews 2000, 1, (1), 1-21.

11. Malinverno, G.; Pantini, G.; Bootman, J., Safety evaluation of perfluoropolyethers, liquid polymers used in barrier creams and other skin-care products. Food and Chemical Toxicology 1996, 34, (7), 639-650.

12. Jang, H. D.; Kim, S.-K.; Kim, S.-J., Effect of Particle Size and Phase Composition of Titanium Dioxide Nanoparticles on the Photocatalytic Properties. Journal of Nanoparticle Research 2001, 3, (2), 141-147.

13. Carp, O.; Huisman, C. L.; Reller, A., Photoinduced reactivity of titanium dioxide. Progress in Solid State Chemistry 2004, 32, (1-2), 33-177.

14. Schulz, J.; Hohenberg, H.; Pflücker, F.; Gärtner, E.; Will, T.; Pfeiffer, S.; Wepf, R.; Wendel, V.; Gers-Barlag, H.; Wittern, K. P., Distribution of sunscreens on skin. Advanced Drug Delivery Reviews 2002, 54, (Supplement 1), S157-S163.

15. Lee, K. P.; Trochimowicz, H. J.; Reinhardt, C. F., Pulmonary response of rats exposed to titanium dioxide (TiO2) by inhalation for two years. Toxicology and Applied Pharmacology 1985, 79, (2), 179-192.

16. Wang, K.-H.; Hsieh, Y.-H.; Ko, R.-C.; Chang, C.-Y., Photocatalytic degradation of wastewater from manufactured fiber by titanium dioxide suspensions in aqueous solution. Environment International 1999, 25, (5), 671-676.

17. Xi, W.; Geissen, S.-u., Separation of titanium dioxide from photocatalytically treated water by cross-flow microfiltration. Water Research 2001, 35, (5), 1256-1262.

18. Ahn, Y.; Yoon, J.-Y.; Baek, C.-W.; Kim, Y.-K., Chemical mechanical polishing by colloidal silica-based slurry for micro-scratch reduction. Wear 2004, 257, (7-8), 785-789.

19. Basim, G. B.; Moudgil, B. M., Effect of Soft Agglomerates on CMP Slurry Performance. Journal of Colloid and Interface Science 2002, 256, (1), 137-142.

20. Manivannan, R.; Ramanathan, S., Role of abrasives in high selectivity STI CMP slurries. Microelectronic Engineering 2008, 85, (8), 1748-1753.

21. Xu, S.; Liu, J.; Sun, Z.; Zhang, P., A novel inverse method for determining the refractive indices of medium and dispersed particles simultaneously by turbidity measurement. Journal of Colloid and Interface Science 2008, 326, (1), 110-116.

22. Lin, W.; Galletto, P.; Borkovec, M., Charging and Aggregation of Latex Particles by Oppositely Charged Dendrimers. Langmuir 2004, 20, (18), 7465-7473.

23. Holthoff, H.; Egelhaaf, S. U.; Borkovec, M.; Schurtenberger, P.; Sticher, H., Coagulation Rate Measurements of Colloidal Particles by Simultaneous Static and Dynamic Light Scattering. Langmuir 1996, 12, (23), 5541-5549.

24. Sun, Z.; Liu, J.; Xu, S., Study on Improving the Turbidity Measurement of the Absolute Coagulation Rate Constant. Langmuir 2006, 22, (11), 4946-4951.

25. Liu, J.; Xu, S.; Sun, Z., Toward an Understanding of the Turbidity Measurement of Heterocoagulation Rate Constants of Dispersions Containing Particles of Different Sizes. Langmuir 2007, 23, (23), 11451-11457.

26. Lichtenbelt, J. W. T.; Ras, H. J. M. C.; Wiersema, P. H., Turbidity of coagulating lyophobic sols. Journal of Colloid and Interface Science 1974, 46, (3), 522-527.

27. Schröer, W.; Köser, J.; Kuhnen, F., Light-scattering in turbid fluids: The single-scattering intensity. Journal of Molecular Liquids 2007, 134, (1-3), 40-48.

28. Glover, S. M.; Yan, Y.-d.; Jameson, G. J.; Biggs, S., Bridging flocculation studied by light scattering and settling. Chemical Engineering Journal 2000, 80, (1-3), 3-12.

29. Morais, I. s. P. A.; Rangel, A. n. O. S. S., Turbidimetric and Nephelometric Flow Analysis: Concepts and Applications. Spectroscopy Letters 2006, 39, (6), 547-579.

30. R. J. Davies-Colley, D. G. S., Turbidity Sediment, And Water Clarity: A Review. Journal of the American Water Resources Association 2001, 37, (5), 1085-1101.

31. Caron, P.; Faucompré, B.; Membrey, F.; Foissy, A., A new white light photosedimentometer for solid-liquid dispersion study: device description, stability and settling behaviour. Powder Technology 1996, 89, (2), 91-100.

32. Caflisch, R., Sedimentation of a random dilute suspension. In Macroscopic Modelling of Turbulent Flows, 1985; pp 14-23.

33. Brown, P. P.; Lawler, D. F., Sphere Drag and Settling Velocity Revisited. Journal of Environmental Engineering 2003, 129, (3), 222-231.

34. Wu, R. M.; Lee, D. J., Hydrodynamic drag force exerted on a moving floc and its implication to free-settling tests. Water Research 1998, 32, (3), 760-768.

35. Chen, S. B.; Cai, A., Hydrodynamic Interactions and Mean Settling Velocity of Porous Particles in a Dilute Suspension. Journal of Colloid and Interface Science 1999, 217, (2), 328-340.

36. Coutinho, C. A.; Gupta, V. K., Formation and properties of composites based on microgels of a responsive polymer and TiO2 nanoparticles. Journal of Colloid and Interface Science 2007, 315, (1), 116-122.

37. Chen, L. X.; Rajh, T.; Wang, Z.; Thurnauer, M. C., XAFS Studies of Surface Structures of TiO2 Nanoparticles and Photocatalytic Reduction of Metal Ions. J. Phys. Chem. B 1997, 101, (50), 10688-10697.

38. Datye, A. K.; Riegel, G.; Bolton, J. R.; Huang, M.; Prairie, M. R., Microstructural Characterization of a Fumed Titanium Dioxide Photocatalyst. Journal of Solid State Chemistry 1995, 115, (1), 236-239.

39. Litter, M. I., Heterogeneous photocatalysis: Transition metal ions in photocatalytic systems. Applied Catalysis B: Environmental 1999, 23, (2-3), 89-114.

40. Ohno, T.; Sarukawa, K.; Tokieda, K.; Matsumura, M., Morphology of a TiO2 Photocatalyst (Degussa, P-25) Consisting of Anatase and Rutile Crystalline Phases. Journal of Catalysis 2001, 203, (1), 82-86.

41. Karg, M.; Pastoriza-Santos, I.; Rodriguez, G.; x; lez, B.; von Klitzing, R.; Wellert, S.; Hellweg, T., Temperature, pH, and Ionic Strength Induced Changes of the Swelling Behavior of Pnipam; Copolymer Microgels. Langmuir 2008, 24, (12).

42. Song, M.; Pan, C.; Li, J.; Zhang, R.; Wang, X.; Gu, Z., Blends of TiO2 nanoparticles and poly (N-isopropylacrylamide)-co-polystyrene nanofibers as a means to promote the biorecognition of an anticancer drug. Talanta 2008, 75, (4), 1035-1040.

43. Jia Guo, Organic-Dye-Coupled Magnetic Nanoparticles Encaged Inside Thermoresponsive PNIPAM Microcapsules. Small 2005, 1, (7), 737-743.

44. Han, H. D.; Shin, B. C.; Choi, H. S., Doxorubicin-encapsulated thermosensitive liposomes modified with poly(N-isopropylacrylamide-co-acrylamide): Drug release behavior and stability in the presence of serum. European Journal of Pharmaceutics and Biopharmaceutics 2006, 62, (1), 110-116.

45. Kim, J.; Singh, N.; Lyon, L. A., Displacement-Induced Switching Rates of Bioresponsive Hydrogel Microlenses. Chem. Mater. 2007, 19, (10), 2527-2532.

46. Yueming Zhou, K. J. Y. C. S. L., Gold nanoparticle-incorporated core and shell crosslinked micelles fabricated from thermoresponsive block copolymer of -isopropylacrylamide and a novel primary-amine containing monomer. Journal of Polymer Science Part A: Polymer Chemistry 2008, 46, (19), 6518-6531.

47. Ayi, T.-C.; Tong, J. M.-M.; Lee, P. V.-S. In Optically tunable hydrogel biosensor material, Chemical and Biological Sensing VII, Orlando (Kissimmee), FL, USA, 2006; SPIE: Orlando (Kissimmee), FL, USA, 2006; pp 62180K-8.

48. Cheng, C.-J.; Chu, L.-Y.; Zhang, J.; Wang, H.-D.; Wei, G., Effect of freeze-drying and rehydrating treatment on the thermo-responsive characteristics of poly(N -isopropylacrylamide) microspheres. Colloid & Polymer Science 2008, 286, (5), 571-577.

49. Sonntag, R. C.; Russel, W. B., Structure and breakup of flocs subjected to fluid stresses. I. Shear experiments. Journal of Colloid and Interface Science 1986, 113, (2), 399-413.

50. Singh, R. K.; Roberts, B. R. In On extensive pump handling of chemical-mechanical polishing slurries, Advanced Semiconductor Manufacturing Conference, 2001; 2001; pp 107-113.

51. Park, S.-S.; Cho, C.-H.; Ahn, Y., Hydrodynamic analysis of chemical mechanical polishing process. Tribology International 2000, 33, (10), 723-730.

52. Zhao, Y.; Chang, L., A micro-contact and wear model for chemical-mechanical polishing of silicon wafers. Wear 2002, 252, (3-4), 220-226.

53. Feng, X.; Sayle, D. C.; Wang, Z. L.; Paras, M. S.; Santora, B.; Sutorik, A. C.; Sayle, Yang, Y.; Ding, Y.; Wang, X.; Her, Y.-S., Converting Ceria Polyhedral Nanoparticles into Single-Crystal Nanospheres. Science 2006, 312, (5779), 1504-1508.

54. Park, B.; Lee, H.; Park, K.; Kim, H.; Jeong, H., Pad roughness variation and its effect on material removal profile in ceria-based CMP slurry. Journal of Materials Processing Technology 2008, 203, (1-3), 287-292.

55. Coutinho, C. A.; Mudhivarthi, S. R.; Kumar, A.; Gupta, V. K., Novel ceria-polymer microcomposites for chemical mechanical polishing. Applied Surface Science In Press, Corrected Proof.

56. Mudhivarthi, S. R.; Coutinho, C.; Kumar, A.; Gupta, V., Novel Hybrid Abrasive Particles for Oxide CMP Applications. ECS Transactions 2007, 3, (41), 9-19.